Journal of Sound and Vibration (1997) **200**(5), 729–735

A GRAPHICAL APPROACH TO WAVE PROPAGATION IN A RIGID DUCT

F. Farassat

Fluid Mechanics and Acoustics Division, NASA Langley Research Center, Hampton, Virginia 23681-0001, *U.S.A.*

AND

M. K. Myers

The George Washington University, Joint Institute for Advancement of Flight Sciences, Hampton, Virginia 23681-0001, *U.S.A.*

(*Received* 12 *June* 1996)

1. INTRODUCTION

Acoustic wave propagation through a flow in an infinite duct is a subject that has lately received renewed attention in connection with the design and understanding of the noise characteristics of ducted fan engines. Noise is generated inside the engine by various flow related mechanisms such as rotor wake–stator interaction, and it propagates from its source through the inlet and exhaust ducts. Of course, the ducts of all engines are finite in length, and they are generally of non-uniform cross-sectional area. Nevertheless, the study of acoustic wave propagation in infinite ducts of uniform circular or annular shapes has been very useful to engine designers interested in obtaining practical qualitative and quantitative information. Perhaps the most basic paper on infinite duct acoustic wave propagation is that of Tyler and Sofrin [1]. Many useful results are found in this paper and elsewhere on infinite duct propagation that one must understand in order to explain various aspects of engine noise, even though acoustic analyses of real engines carrying non-uniform flows in finite ducts are considerably more complicated [2, 3].

In this letter we give a graphical representation applicable to wave propagation in an infinite duct carrying a uniformly moving fluid. The representation was first presented by the authors in reference [4]. The graphical approach is easily implemented on a personal computer, and it can be especially useful for those new to the area of duct acoustics. We show that many known results can be derived easily using the graphical method. It involves construction of an ellipse in wavenumber space, the shape of which is dependent only on flow speed. The propagating waves as well as the upstream and downstream wave number vectors are then obtained graphically. In addition, the direction of energy propagation, the mode cut-off concept and the approximate radiation angle for each mode can all be illustrated by graphical construction.

2. GRAPHICAL APPROACH TO WAVE PROPAGATION IN A UNIFORM DUCT WITH FLOW

Consider a duct of uniform circular or annular cross-section carrying a uniform flow at Mach number $M < 1$. The differential equation and the boundary condition for propagation of small pressure perturbations for the hard wall case is

$$\left(\frac{1}{c_0}\frac{\partial}{\partial t} + M\frac{\partial}{\partial x}\right)^2 p' - \nabla^2 p' = 0, \qquad \frac{\partial p'}{\partial r} = 0 \quad \text{(on the wall)}, \tag{1a, b}$$

0022–460X/97/100729 + 07 $25.00/0/sv960691

in which x is the axial co-ordinate along the duct. If cylindrical polar co-ordinates (r, θ, x) are used, and if it is assumed that a complex solution for the acoustic pressure p' exists in the form

$$p' = P(r, \theta, x)\, e^{i\omega t} \tag{2}$$

then the complex amplitude P satisfies the equations

$$(1 - M^2)\frac{\partial^2 P}{\partial x^2} + \nabla_2^2 P - 2ikM\frac{\partial P}{\partial x} + k^2 P = 0, \qquad \frac{\partial P}{\partial r} = 0 \quad \text{(on the wall)}, \tag{3a, b}$$

in which $k = \omega/c_0$ and ∇_2^2 is the two-dimensional Laplacian in polar co-ordinates.

Let $k_a(m, n)$ and $k_r(m, n)$ be the axial and radial wavenumbers for the mth circumferential and nth radial mode. Now considering a circular duct of radius R, the solution of equation (1) for the mode (m, n) is

$$p' = A_{mn} J_m[k_r(m, n)r] \exp i[\omega t - m\theta - k_a(m, n)x], \tag{4}$$

where the $k_r(m, n)$ are obtained as the roots of

$$J'_m[k_r(m, n)R] = 0, \tag{5}$$

numbered in consecutive order by $n = 1, 2, 3, \ldots$. Here $J_m(\cdot)$ is a Bessel function of the first kind of order m. Let $\beta^2 = 1 - M^2$. Then $k_a(m, n)$ is given from equations (3) and (4) by

$$k_a(m, n) = (k/\beta^2)[-M \pm \sqrt{1 - [\beta k_r(m, n)/k]^2}] = (k/\beta^2)[-M \pm \sqrt{1 - 1/\beta_{mn}^2}], \tag{6}$$

in which $m = 0, 1, 2, \ldots$. We have defined the cut-off ratio β_{mn} as

$$\beta_{mn} = k/\beta k_r(m, n). \tag{7}$$

It then follows that the mode (m, n) is propagating if $\beta_{mn} > 1$ and decaying if $\beta_{mn} < 1$.

In preparation for the graphical approach, we write equation (6) as

$$\frac{(\tilde{k}_1 + M/\beta^2)^2}{1/\beta^4} + \frac{\tilde{k}_2^2}{1/\beta^2} = 1, \tag{8}$$

where $\tilde{k}_1 = k_a/k$ and $\tilde{k}_2 = k_r/k$. For use later, we note that equation (8) can also be expressed as

$$\tilde{k}_1^2 + \tilde{k}_2^2 = (1 - M\tilde{k}_1)^2. \tag{9}$$

Equation (8) is an ellipse in the variables $(\tilde{k}_1, \tilde{k}_2)$ with center at $(-M/\beta^2, 0)$ and with semi-major and semi-minor axes $1/\beta^2$ and $1/\beta$, respectively. The ellipse depends only on M. It intersects the $\tilde{k}_1$-axis at $\tilde{k}_1 = 1/(1 + M) > 0$ and $\tilde{k}_1 = -1/(1 - M) < 0$. It always intersects the $\tilde{k}_2$-axis at $\tilde{k}_2 = \pm 1$. In Figure 1 is shown the ellipse described by equation (8) for flow Mach number $M = 0{\cdot}8$. Note that, for $M = 0$, equation (8) gives a circle of unit radius in the $\tilde{k}_1\tilde{k}_2$-plane with its center at the origin. We now use this ellipse to study some aspects of wave propagation in a circular duct.

2.1. *Propagating and decaying modes*

In Figure 2 it is shown how one determines the propagating and decaying modes. On different vertical axes, each corresponding to a circumferential mode m, plot the solutions of equation (5); i.e., $k_r(m, n)/k$ for $n = 1, 2, \ldots$. Draw horizontal lines as shown in this figure for $m = 0$. If these lines intersect the ellipse, the mode (m, n) is a propagating mode. Otherwise, the mode is decaying. In general, we obtain two values for k_a, which we denote as k_{a+} and k_{a-}. In Figure 2 we have shown $k_{a+}(0, 3)/k$ and $k_{a-}(0, 3)/k$. Note that k_a

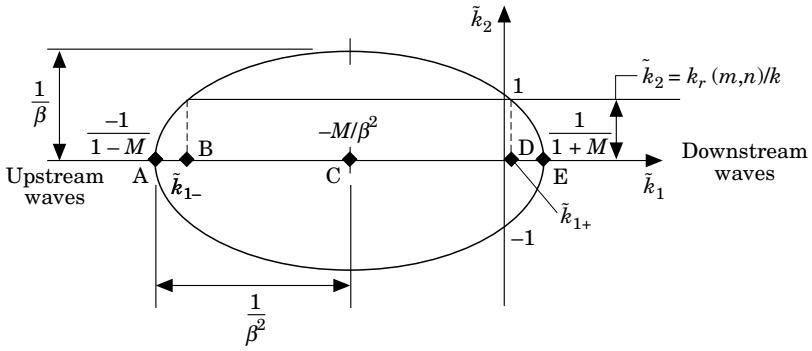

Figure 1. The ellipse of the wavenumber vector described by equation (8); $\tilde{k}_1 = k_a/k$, $\tilde{k}_2 = k_r/k$, $M = 0{\cdot}8$. Corresponding to each propagating wave with a given $\tilde{k}_2$, two axial wavenumbers $\tilde{k}_{1+}$ and $\tilde{k}_{1-}$ are obtained.

determines the axial phase speed of the mode (m, n). The k_{a+} mode is generally called the downstream mode, but any propagating k_{a+} mode for which $k_r/k > 1$ actually moves in the negative x direction; this is the case with $k_{a+}(0, 3)$ in Figure 2. The relationship of the phase speed of the mode to the velocity of energy propagation in the mode will be discussed below.

2.2. *Mode cut-off and energy flow*

When the cut-off ratio β_{mn} is equal to unity, $\tilde{k}_2 = 1/\beta$. Since the semi-minor axis of the ellipse in the $\tilde{k}_1\tilde{k}_2$-plane is $1/\beta$, the axial wave number corresponding to $\tilde{k}_2 = 1/\beta$ is $\tilde{k}_1 = k_a/k = -M/\beta^2$. The wavenumber vector for the cut-off condition at $M = 0{\cdot}8$ is shown in Figure 3. It indicates that the k_{a+} wave propagates upstream. To discover what is special about the wavenumber vector at cut-off, we consider the acoustic energy flux vector for the modal solution given by equation (4).

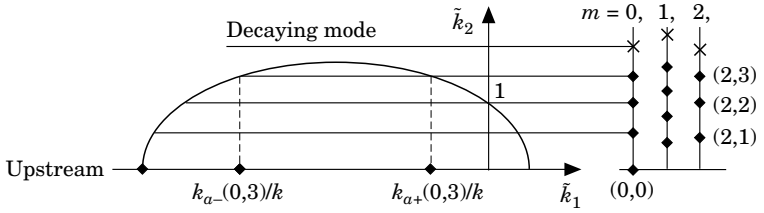

Figure 2. The determination of propagating and decaying waves. Each vertical line on the right corresponds to the circumferential mode. $M = 0{\cdot}8$. ◆, Propagating; ×, decaying.

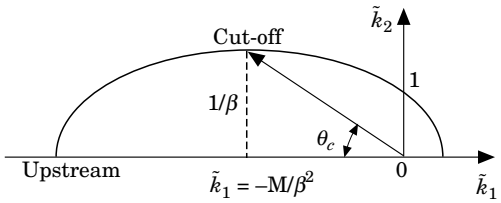

Figure 3. The wavenumber vector at cut-off, $M = 0{\cdot}8$.

For isentropic disturbances in a uniform flow at velocity $\mathbf{V}$, the acoustic energy flux vector can be written as [5]

$$\mathbf{W} = (p' + \rho_0 \mathbf{V} \cdot \mathbf{u}')\left(\mathbf{u}' + \frac{p'}{\rho_0 c_0^2}\mathbf{V}\right) = (p' + \rho_0 c_0 \mathbf{M} \cdot \mathbf{u}')\left(\mathbf{u}' + \frac{p'}{\rho_0 c_0}\mathbf{M}\right). \tag{10}$$

In equation (10), $\mathbf{u}'$ is the acoustic particle velocity corresponding p', ρ_0 is the density of the undisturbed flow, and $\mathbf{M}$ is the flow Mach number vector $\mathbf{V}/c_0$. The (primed) disturbance quantities are the actual (real) acoustic pressure and velocity. For an acoustic field represented in the complex form of equation (4), the linearized momentum equation gives

$$\mathbf{u}' = \frac{-\nabla p'}{\mathrm{i}\rho_0 c_0 k(1 - M\tilde{k}_1)} = \frac{\tilde{k}_1 p'}{\rho_0 c_0 (1 - M\tilde{k}_1)}\mathbf{e}_1 + \mathbf{u}_2', \tag{11}$$

in which $\mathbf{e}_1$ is the unit vector along the x direction and $\mathbf{u}_2'$ is the projection of $\mathbf{u}'$ on the cross-sectional plane of the duct. Thus, for the single-mode complex solution given by equation (4), we have

$$\mathbf{W} = \mathrm{Re}\left[\frac{p'}{1 - M\tilde{k}_1}\right] \cdot \mathrm{Re}\left[\frac{\beta^2\tilde{k}_1 + M}{\rho_0 c_0 (1 - M\tilde{k}_1)} p'\mathbf{e}_1 + \mathbf{u}_2'\right]. \tag{12}$$

Here $\mathrm{Re}\,[\,\cdot\,]$ denotes the real part of $[\,\cdot\,]$. We see from equation (12) that at the cut-off condition, $\tilde{k}_1 = -M/\beta^2$, the axial component of the acoustic energy flux vanishes: $\mathbf{W}$ is normal to the wall and no energy propagates along the duct axis. Equation (12) also shows that the modal intensity, which is the time-average of $\mathbf{W}$, will have an axial component proportional to $(\beta^2\tilde{k}_1 + M)|p'|^2$. This is positive for all $\tilde{k}_1 > -M/\beta^2$. Hence, a mode such as $k_{a+}(0, 3)$ in Figure 2 always carries power in the positive x direction even though its axial phase speed is negative.

The cut-off of axial energy flux can also be exhibited graphically on the wavenumber ellipse, although only approximately for a circular duct (the interpretation is exact for ducts of rectangular cross-section). For this purpose we use the large argument approximation of the Bessel function,

$$\mathrm{J}_m(k_r r) \approx \sqrt{\frac{2}{\pi k_r r}} \cos(k_r r - \psi_m), \tag{13}$$

with $\psi_m = \pi/4 + m\pi/2$ to approximate p' by

$$p' \approx \frac{A_{mn}}{2}\sqrt{\frac{2}{\pi k_r r}}\{\exp \mathrm{i}[\omega t - m\theta - k_a x - k_r r - \psi_m] + \exp \mathrm{i}[\omega t - m\theta - k_a x + k_r r + \psi_m]\}. \tag{14}$$

We see that, for sufficiently large $k_r r$ at any fixed θ, p' can be considered to be the sum of two progressing waves in (x, r), the phases of which are

$$\phi_\pm = \omega t - k_a x \mp k_r r = k(c_0 t - \tilde{k}_1 x \mp \tilde{k}_2 r). \tag{15}$$

The unit vectors normal to these planar phase surfaces are $\mathbf{n}_\pm = -\nabla\phi_\pm/|\nabla\phi_\pm|$, or

$$\mathbf{n}_\pm = \frac{(\tilde{k}_1, \pm\tilde{k}_2)}{\sqrt{\tilde{k}_1^2 + \tilde{k}_2^2}} = \frac{(\tilde{k}_1, \pm\tilde{k}_2)}{\mathrm{p}1 - M\tilde{k}_1}, \tag{16}$$

where we have used equation (9). Now if we invert equation (16) to express the wavenumber vector $\mathbf{k}_\pm = (\tilde{k}_1, \pm\tilde{k}_2)$ in terms of $\mathbf{n}_\pm$, we obtain

$$\mathbf{k}_\pm = \mathbf{n}_\pm/(1 + \mathbf{M}\cdot\mathbf{n}_\pm). \tag{17}$$

If we use equation (17) in equation (15) we find that

$$\phi_\pm = \omega t - \frac{k\mathbf{n}_\pm\cdot\mathbf{r}}{1 + \mathbf{M}\cdot\mathbf{n}_\pm}, \tag{18}$$

where $\mathbf{r}$ is the position vector (x, r) in the plane of constant θ. The phases in equation (18) are precisely those of a pure plane wave propagating in the directions $\mathbf{n}_\pm$ in the x–r plane. The phase speeds of these waves are, from equation (18), $c_0(1 + \mathbf{M}\cdot\mathbf{n}_\pm)$.

If the approximation is viewed locally and variations in the geometric factor $r^{-1/2}$ are ignored, then equation (14) implies that at points sufficiently close to the duct wall at least the higher order n modes can be interpreted as being a sum of two interfering plane waves propagating in the directions $\mathbf{n}_\pm$. For each of these separately, the relation $\mathbf{u}' = p'\mathbf{n}/\rho_0 c_0$ holds so that the energy flux associated with each is given from equation (10) by

$$\mathbf{W} = \frac{p'^2}{\rho_0 c_0^2}(1 + \mathbf{M}\cdot\mathbf{n})(c_0\mathbf{n} + \mathbf{V}). \tag{19}$$

The last factor in equation (19) is the energy propagation velocity, or the group velocity $\mathbf{V}_G$, of the plane wave:

$$\mathbf{V}_G = c_0\mathbf{n} + \mathbf{V} = c_0(\mathbf{n} + \mathbf{M}), \tag{20}$$

and it is this quantity associated with the approximate plane wave representation of the duct modes that is convenient to consider in conjunction with the wavenumber ellipse.

If we again refer to Figure 3, we see that at cut-off the component of $\mathbf{V}_G$ in the x direction is

$$\mathbf{V}_G\cdot\mathbf{e}_1 = c_0(-\cos\theta_c + M) = c_0(-M + M) = 0. \tag{21}$$

Here we have used the fact that, as seen from Figure 3, $\tan\theta_c = \beta/M$ and thus $\cos\theta_c = M$, where θ_c is the angle that $\tilde{k}$ at the cut-off condition makes with the $\tilde{k}_1$-axis. Equation (21) means that the acoustic energy flux vector is normal to the wall and no energy is propagated along the axis.

To find the direction of group velocity in our graphical construction, follow the vector diagram of Figure 4. This diagram is in the $\tilde{k}_1\tilde{k}_2$-plane, so that $\mathbf{M}$ must be scaled up to $\mathbf{M}/\beta^2$ to obtain the direction of the group velocity as shown in this plane. From the figure, it is clear that at the cut-off condition the group velocity points upward, and thus the energy flux vector is normal to the wall.

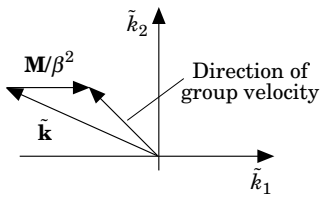

Figure 4. The diagram for finding the direction of group velocity in the $\tilde{k}_1\tilde{k}_2$-plane.

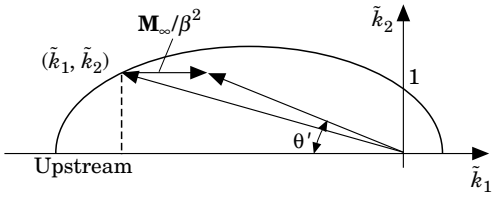

Figure 5. The diagram for construction of θ', the angle of the main radiation lobe from an inlet, as proposed by Rice *et al*. [6]. The ellipse is based on the duct Mach number ($M = 0{\cdot}8$) and the flight Mach number is M_∞.

2.3. *The angle of the main lobe of radiation from an inlet*

Rice, *et al*. [6] have proposed a rule for finding the angle of the main lobe of radiation from an inlet where the duct Mach number is M and the inflow Mach number (flight speed) is M_∞. By our graphical method we can give a simple interpretation of their rule as follows. Intuitively, it is obvious that the phase velocity of a radiating mode at the inlet should be based on M, the duct flow Mach number. However, the angle of the main lobe of radiation is in the direction of the group velocity using $\mathbf{M}_\infty$ instead of $\mathbf{M}$ in Figure 4. This construction is shown in Figure 5. Here θ' is the sought angle. The mathematical reasoning is as follows. Remembering that $\tilde{k}_1 < 0$, we have, from Figure 5,

$$\tan\theta' = \frac{\tilde{k}_2}{\tilde{k}_1 + M_\infty/\beta^2} = \frac{\beta}{|(M_\infty - M)\beta_{mn} - \sqrt{\beta_{mn}^2 - 1}|}, \tag{22}$$

where β_{mn} is the cut-off ratio. This is equivalent to the expression that Rice *et al*. [6] gave for $\cos\theta'$.

2.4. *Other results*

One can easily show graphically some other known results. One is the following: if a mode (m, n) propagates for $M = M_1$, then it will propagate for duct Mach number $M_2 > M_1$. The proof is simple. From Figure 6 the semi-minor axis of the ellipse for M_2 is $1/\beta_2$, where $\beta_2 = \sqrt{1 - M_2^2} < \beta_1 = \sqrt{1 - M_1^2}$. Therefore, $1/\beta_2 > 1/\beta_1$ is the semi-minor axis of the ellipse for M_1. Hence, a horizontal line that intersects the ellipse for $M = M_1$ necessarily intersects the ellipse for $M = M_2$ (see Figure 6).

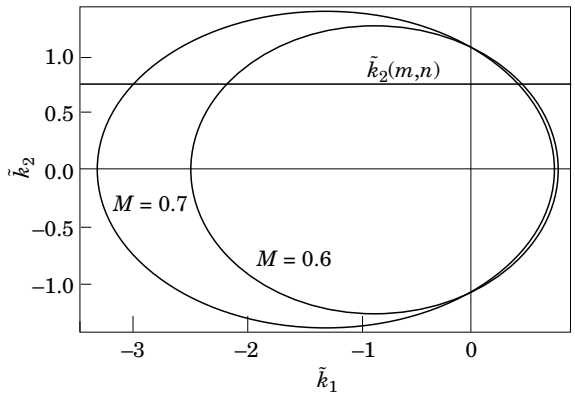

Figure 6. The ellipses for $M = 0{\cdot}6$ and $M = 0{\cdot}7$. Mode (m, n) propagates for $M = 0{\cdot}6$. Therefore, it propagates for $M > 0{\cdot}6$.

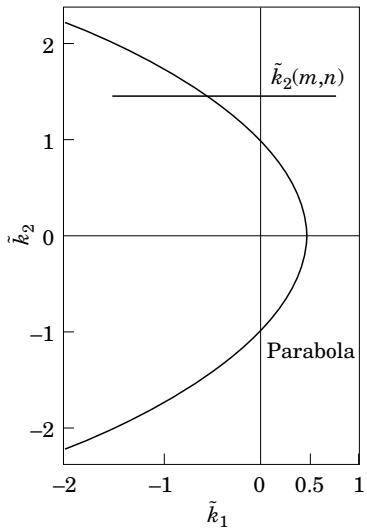

Figure 7. The degenerate ellipse (a parabola) as $M \to 1$. Note that as $\tilde{k}_1 \to -\infty$, we have $\tilde{k}_2 \to \pm\infty$. Any horizontal line intersects the parabola; i.e., all modes propagate.

Another result is that as $M \to 1$ all modes will propagate. Again, the graphical proof is very simple. As $M \to 1$, $\beta \to 0$ and the equation of the ellipse degenerates into the parabola

$$\tilde{k}_2^2 = 1 - 2\tilde{k}_1. \tag{23}$$

The axis of this parabola is the $\tilde{k}_1$-axis and the parabola intersects the $\tilde{k}_1$-axis at $\tilde{k}_1 = 1/2$. The parabola extends to infinity in the $\tilde{k}_2$ direction, so that any horizontal line intersects it (see Figure 7). This means, by our graphical method of discovering propagating modes, that all modes propagate.

We mention here that the ellipse of Figure 1 remains unchanged for two-dimensional, three-dimensional rectangular and annular ducts. Only the values of $\tilde{k}_2$ for the modes, which depend on the duct geometry, will change.

REFERENCES

1. J. M. Tyler and T. G. Sofrin 1962 *SAE Transactions* **70**, 309–332. Axial flow compressor noise studies.
2. A. H. Nayfeh, J. E. Kaiser and B. S. Shaker 1979 *NASA CR*-3109. A wave-envelope anlaysis of sound propagation in non-uniform circular ducts with compressible mean flows.
3. K. Uenishi and M. K. Myers 1984 *American Institute of Aeronautics and Astronautics Journal* **22**, 1242–1248. Two-dimensional acoustic field in a nonuniform duct carrying compressible flow.
4. F. Farassat and M. K. Myers 1996 *AIAA Paper* 96-1677. A study of wave propagation in a duct and mode radiation.
5. M. K. Myers 1986 *Journal of Sound and Vibration* **109**, 277–284. An exact energy corollary for homentropic flow.
6. E. J. Rice, M. F. Heidmann and T. G. Sofrin 1979 *AIAA Paper* 79-0183. Modal propagation angles in a cylindrical duct with flow and their relation to sound radiation.